DESIGN CONSIDERATIONS FOR A TWO-DISTRIBUTED-JUNCTION TUNING CIRCUIT

Yoshinori UZAWA[1)], Masanori TAKEDA[1)], Akira KAWAKAMI[1)], Zhen WANG[1)], and Takashi NOGUCHI[2)]

1) Kansai Advanced Research Center, National Institute of Information and Communications Technology
588-2 Iwaoka, Iwaoka-cho, Nishi-ku, Kobe 651-2492, Japan
e-mail: uzawa@nict.go.jpT
2) Nobeyama Radio Observatory, National Astronomical Observatory of Japan
Nobeyama, Nagano 384-1305, Japan

Abstract

We describe a novel method of designing a tuning circuit with two half-wave distributed junctions separated by a half-wavelength microstripline, which analytically determines the circuit parameters such as the minimum current density of the junctions and the characteristic impedances of the distributed junctions and the microstripline. The tuning circuit was approximated by simple transmission theory and then simplified with ideal circuit components for analysis. We applied Chebyshev's band-pass filter theory, in part, to optimize the circuit design. The analytical results revealed that a high characteristic-impedance ratio between the distributed junctions and the microstripline is necessary to obtain broadband matching using low-current-density junctions. The experimental results for all-NbN SIS mixers we designed with this method demonstrated double-sideband (DSB) receiver-noise temperatures of 6-10 quanta from 710 to 810 GHz for a mixer with a current density of only 4 kA/cm^2 (estimated $\omega C_J R_N$ product of 37 at 750 GHz). The RF bandwidth was broader than that of a conventional full-wave distributed SIS mixer with the same current density.

1. Introduction

The quality of superconductor-insulator-superconductor (SIS) junctions strongly influences mixer noise. In general, the subgap leakage current of the junction tends to become large for high current density, which degrades mixer performance. It is better to use SIS junctions with a current density as low as possible to achieve low noise. However, SIS junctions have large specific capacitances C_S, of say 100 fF/μm^2 for typical junctions such as Nb/AlOx/Nb and NbN/AlN(or MgO)/NbN, which roughly limit the operational fractional bandwidth, $\Delta f/f_0$, to $1/\omega C_J R_N$ using a conventional tuning circuit design, where ω, C_J, and R_N are the signal angular frequency, geometrical junction capacitance, and normal resistance of the junction, respectively. To achieve a fractional bandwidth of 20%, for example, the $\omega C_J R_N$ should be 5 at the center frequency. The $\omega C_J R_N$ product is related to the current density, J_C, according to $\omega C_S I_C R_N / J_C$. Appling this relation to the highest band of the Atacama Large Millimeter Array (ALMA), which is the 787-950 GHz (band 10), high-current-density junctions of about 20 kA/cm^2 for Nb and 40 kA/cm^2 for NbN are necessary. Consequently, it is difficult to achieve ultra-low noise for the ALMA band 10 using a conventional tuning circuit faced with the expected low quality of SIS junctions with high current densities [1].

We previously proposed a novel tuning circuit with two half-wave distributed SIS junctions and theoretically and experimentally demonstrated that its performance enables a fractional bandwidth to be obtained that is broader than $1/\omega C_J R_N$ [2, 3]. Although the design principle behind the tuning circuit was founded on the idea of efficient reactance compensation for open-ended distributed junctions, the circuit designs were produced by varying many circuit parameters, through trial and error, to achieve optimization. Whether the tuning circuit was really optimized using the SIS junctions with the minimum current density was not certain. In this paper, we will explain that the circuit parameters can uniquely be determined with the new design method when the fractional bandwidth and maximum tolerable value for the reflection coefficient between the source and tuning circuit are given as well as filter design theory. The minimum current density of the junctions derived by the design method was much smaller than that of SIS junctions with a conventional tuning circuit. We also present experimental results on a comparison between the two-distributed-junction and the conventional tuning circuit using NbN/MgO/NbN tunnel junctions and microstriplines.

2. Design method

Figure 1 (a) illustrates a two-distributed-junction tuning circuit, in which Z_J, γ_J ($= \alpha_J + j\beta_J$), and d_J respectively represent the characteristic impedance, propagation constant (α_J is the attenuation constant due to quasi-particle loss and β_J is the phase constant below the gap frequency), and length of the distributed junctions. As the microstripline between the junctions is treated as a loss-free transmission line with a characteristic impedance of Z_m and a length of d_m, the propagation constant is described by only a phase constant of β_m below the gap frequency. It looks like a band-pass filter structure consisting of low (distributed junctions) and high (microstripline) impedance sections when $\beta_J d_J$ and $\beta_m d_m$ are chosen to be π at center frequency. The difference in design between an ordinary band-pass filter and the tuning circuit is as follows:

1) Transmission lines composed of the tuning circuit have loss, but the filter circuit is loss free.
2) According to 1), the input and output impedances may be taken to have different values for the tuning circuit, but the same impedances for the filter circuit.

Therefore, we assumed a source impedance of Z_S, which can be any value to optimize the circuit. This assumption is reasonable when a quarter-wave transformer is added to the tuning circuit. Once Z_S is decided by optimization, then this value may easily be transformed to another impedance level that for a waveguide or quasi-optical antenna feed points by using the quarter-wave transformer.

Let us now investigate how to find the optimal solution so that the current density of the junctions is minimized under the design conditions of a fractional bandwidth and a maximum tolerable value for the reflection coefficient in the band between the circuit and Z_S. If the distributed junction has relatively low loss satisfying the following conditional equation

$$\sin(\alpha_J d_J) \cong \alpha_J d_J, \qquad (1)$$

the open-ended distributed junction is described by a loss-free transmission line end-loaded with pure resistance [2]. Another condition expressed by

$$\alpha_J d_J \tan(\beta_J d_J) << 1 \qquad (2)$$

may be satisfied around $\beta_J d_J = \pi$. Using these conditions, the circuit including loss, in part, (Fig. 1 (a)) is simplified with ideal circuit components of loss-free transmission lines and pure resistance as we can see in Fig. 1 (b). Normalizing the impedances to a terminating resistance of $R_L = Z_J/(\alpha_J d_J)$, the circuit in (b) is written as Fig.1 (c). The circuit observed from a-a' toward the load in the figure is just like a 3-section band-pass-filter structure for an input source impedance of unity (the output terminating impedance is now also unity). This part can be designed with the Chebyshev's band-pass filter theory [4]. The question is how

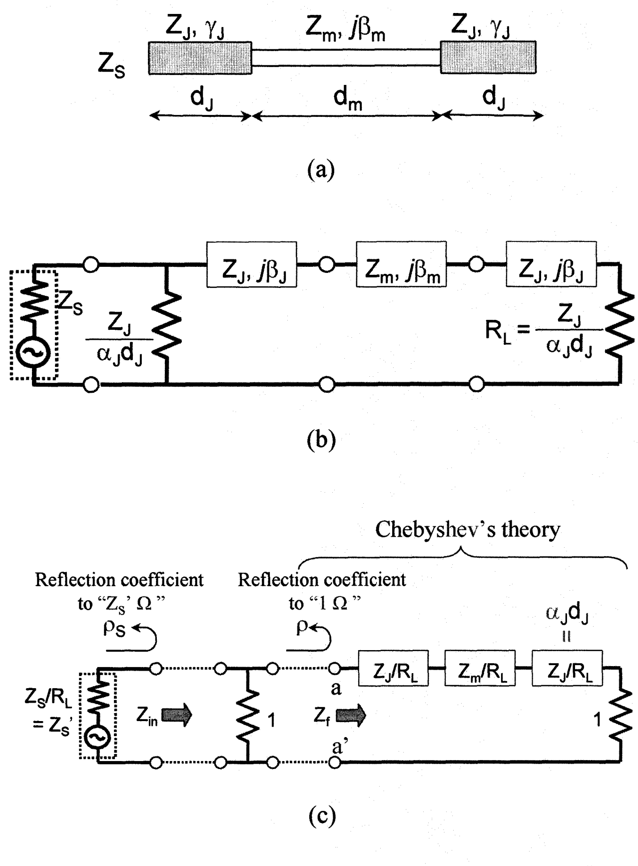

Fig. 1. (a) Diagram of tuning circuit with two half-wave distributed junctions connected by microstripline. (b) Simplified circuit model of tuning circuit. (c) Method of analyzing to optimize circuit parameters.

do we design Chebyshev filter to minimize the current density in the junctions?

The normalized characteristic impedance of the junctions equals $\alpha_J d_J$, which is the attenuation of the distributed junctions in Np. Since the guided wavelength in the distributed junction is almost independent of the junction current density for the same geometrical configuration, the normalized characteristic impedance of the junctions is dependent on the attenuation constant, α_J. Therefore, $\alpha_J d_J$ becomes lower along with decreasing current density, and this value is much less than unity because of the conditional Eq. 1. According to 3-section filter theory, the maximum tolerable value of the reflection coefficient should be large, when the impedance ratio between the terminating load and low impedance section is large. Therefore, to find the minimum current density, the maximum tolerable value in designing Chebyshev filter should be as large as possible under the given design conditions between Z_S and the tuning circuit, as previously mentioned. To find the solution mathematically, we denote the normalized input impedance of the filter as Z_f and the reflection coefficient as ρ, as shown in Fig. 1 (c). It is well known that the relation between Z_f and ρ is

$$\rho = \left| \frac{1 - Z_f}{1 + Z_f} \right| \tag{3}$$

and

$$Z_f = \frac{1 \pm \rho}{1 \mp \rho}. \tag{4}$$

Therefore, the normalized input impedance of the tuning circuit, Z_{in}, as represented in Fig. 1 (c) becomes

$$Z_{in} = \frac{1 \pm \rho}{2}. \tag{5}$$

The maximum reflection coefficient should be below ρ_S as one of the design conditions, hence the conditional equation using the normalized source impedance of Z_S' is obtained by

$$\rho_S \le \left| \frac{Z_S' - Z_{in}}{Z_S' + Z_{in}} \right|. \tag{6}$$

Accordingly, ρ is now written as a function of Z_S'. Thus, we can simultaneously find Z_S' and ρ so that ρ is maximized under the conditions. The actual design procedure is explained in the following example.

Design example:

Consider the design of a tuning circuit with a fractional bandwidth of 20% and having a reflection coefficient of 0.314 or less (-10 dB matching) in the tuning band. Plotting using Eqs.5 and 6 in the Z_S'-ρ plane (Fig. 2), the hatched area is valid for $\rho_S < 0.314$. From this graph, we can obtain $\rho = 0.58$ as the maximum value when $Z_S' = 0.41$. According to Chebyshev's theory, we can hereby easily design an ordinary 3-section band-pass filter for a maximum tolerable reflection coefficient of 0.58 with a fractional bandwidth of 20%. Figure 3 shows the calculated results based on theory. The details on the method to determine the circuit parameters are described elsewhere [4]. Thus, we theoretically determined the impedance ratio of $R_L:Z_J(=\alpha_J d_J):Z_m:Z_S$ = 1:0.12:2.69:0.41 in Fig. 1 (b). This result tells us that the characteristics impedance of the micriostripline should be high

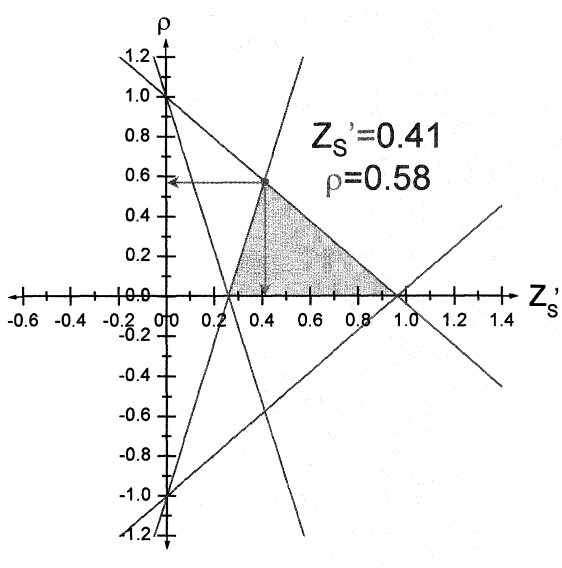

Fig. 2. Reflection coefficient ρ as a function of normalized source impedance Z_S', based on Eqs. 5 and 6. Hatched area indicates design condition of $\rho_S < 0.314$.

compared to those of the distributed junctions. Since it is difficult to achieve high characteristic impedance above 30 Ω using an ordinary configuration of superconducting microstriplines, the characteristic impedance of the distributed junctions should be less than 2 Ω.

Using the derived impedance ratio, we calculated the frequency characteristics of the tuning circuit as plotted in Fig. 4. Figure 4 (a) is a Smith chart plot and (b) is plots the return loss in the tuning circuit. The frequency is normalized at center frequency. From (a), we can see that the designed tuning circuit optimally achieved −10 dB matching with the 20% bandwidth as we expected. As we can see from (b), the normalized source impedance for the tuning circuit was set to less than half the impedance of the terminating load, which made it possible to maximize the reflection coefficient in filter design under a circuit design condition of $\rho_S <$ 0.314. Thus, we found the minimum value for $\alpha_J d_J$. The minimum current density of the distributed junctions can be derived from $\alpha_J d_J = 0.12$. Since the half-wavelength d_J is dependent on SIS junction parameters such as the specific capacitance and the penetration depth of the superconductors, we derived the current density in the actual mixer design based on NbN.

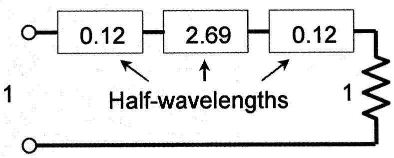

Fig. 3. Circuit parameters determined by ordinary Chebyshev's theory for conditions of $\rho < 0.58$ and $\Delta f/f_0 = 20\%$.

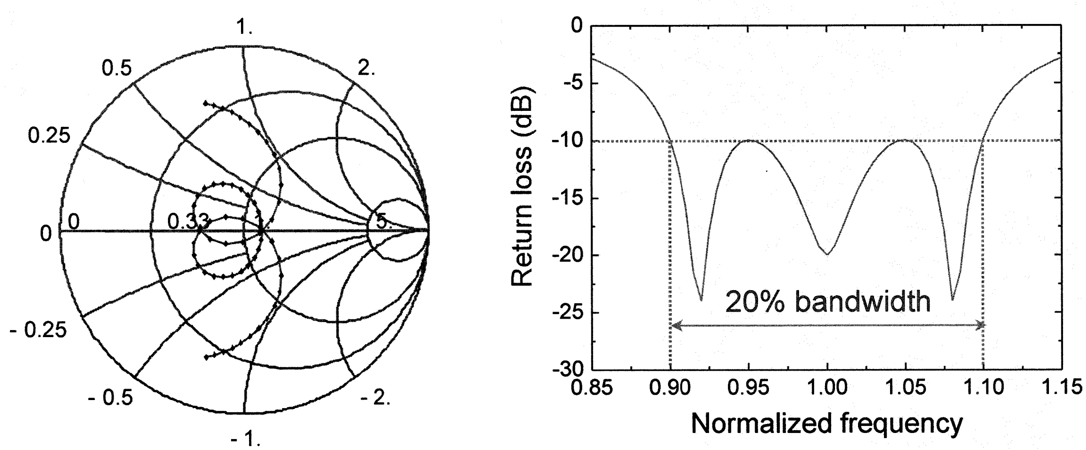

(a) (b)

Fig. 4. (a) Smith chart plot and (b) return loss plot of tuning circuit as a function of normalized frequency.

3. Mixer design

A quasi-optical coupling structure with an MgO substrate lens and a planar twin-slot antenna was used for the mixer input [5]. The feed point of the antenna was centrally positioned using coplanar waveguide transmission lines as can be seen in Fig. 5 (a). A tuning circuit was integrated with one side of the lines as its ground plane. The optical micrograph in Fig. 5 (b) shows that the tuning circuit consisted of two half-wave NbN/MgO/NbN tunnel junctions and NbN/MgO/NbN microstriplines grown epitaxially on a single-crystal MgO substrate [6, 7]. The circuit was connected to the feed point by a quarter-wave impedance transformer. To compare its performance with that of a conventional tuning circuit, we also prepared full-wave distributed junction mixers on the same substrates as seen in Fig. 5 (c).

We designed the tuning circuit to have a center frequency of 870 GHz and a fractional bandwidth of ~20% (ALMA Band 10) with −10 dB matching. The parameters used in our design process are listed in Table 1. The specific capacitance of the NbN/MgO/NbN junctions was assumed to be the same as that of NbN/AlN/NbN

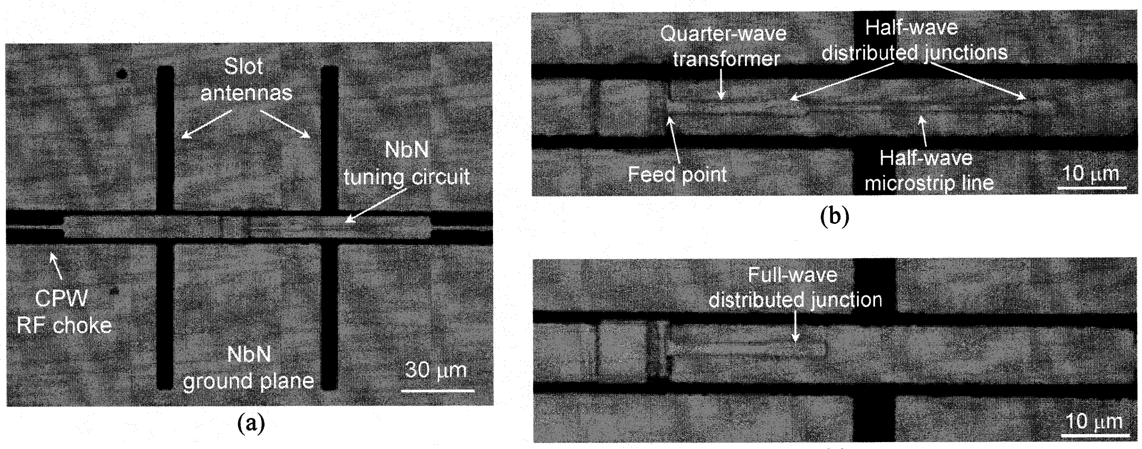

Fig. 5. Optical micrographs of (a) twin-slot antenna mixer, (b) novel tuning circuit with two half-wave SIS junctions, and (c) conventional tuning circuit with full-wave SIS junction.

junctions because the dielectric constants of their tunnel barriers were similar [8]. The method of calculating the characteristic impedance and propagation constant of the distributed SIS junctions, including the overhanging structure with the NbN/MgO/NbN microstrip line for wiring the SIS junctions, is described elsewhere [9]. The surface impedances of the upper and lower electrodes were calculated using the Mattis-Bardeen theory of the anomalous skin effect [10]. We derived the theoretical minimum current density according to the description in the former section. Figure 6 plots the dependence of attenuation ($\alpha_J d_J$) on current density for a distributed NbN junction with a width of 1 μm at a center frequency of 870 GHz. From this figure, the current density to satisfy $\alpha_J d_J$ = 0.12 is about 16 kA/cm^2 (calculated $\omega C_J R_N$ product of about 13) which is much lower than the 40 kA/cm^2 needed for conventional tuning-circuit design ($\omega C_J R_N$ product of about 5).

The diagram in Fig. 7 shows the tuning circuit we designed assuming a constant source impedance of 65 Ω. The impedance ratio of the circuit was taken to have

Table 1. Design parameters.

NbN gap frequency	1.4 THz
normal state conductivity	1.5 x 10^6 Ω^{-1}m^{-1}
upper electrode thickness	400 nm
lower electrode thickness	200 nm
MgO insulator thickness	200 nm
dielectric constant	9.6
NbN/MgO/NbN $J_C R_N A$ product	3.5 mV
Specific capacitance	71 $J_C^{0.16}$ fF/μm^2
MgO barrier thickness	1 nm

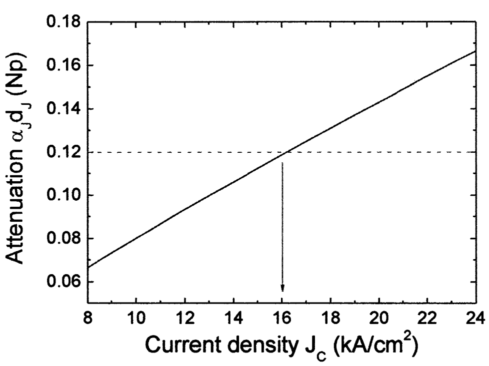

Fig. 6. Attenuation of distributed junction as a function of current density.

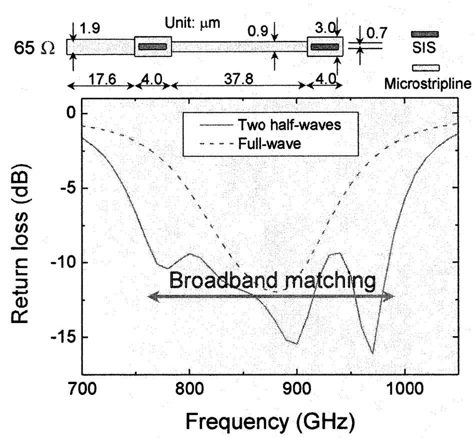

Fig. 7. Layout and theoretical return loss of tuning circuit.

approximately the same values derived above. The return loss of the circuit is also plotted in Fig. 7. A fractional bandwidth of 20% was achieved by using junctions with a current density of 16 kA/cm^2, as was expected theoretically. To compare this bandwidth with that of a conventional tuning method, we calculated the return loss of an SIS mixer with a full-wave junction having the same current density [11]. As we can see in Fig. 7, the fractional bandwidth of the mixer with two half-wave junctions was much broader than that with the full-wave junction.

4. Receiver performance

The mixer chips were fabricated using a process described elsewhere [6, 7]. The critical current density of the junctions was about 4 kA/cm^2, which was measured using other junctions with a large area on the same substrate. The mixer chips were placed on an MgO hyperhemisphere with a 50-μm-thick Kapton-JP anti-reflection cap. The receiver set-up was basically the same as described previously [12], except for the use of a backward-wave oscillator instead of an optically pumped far-infrared laser as the local oscillator (LO) source. The signal and LO power, coupled using a 9-μm-thick Mylar beam splitter, entered the Dewar through a 0.5-mm-thick Teflon vacuum window and Zitex infrared filters cooled to 77 K and 4.2 K, respectively. The intermediate frequency (IF) signal at 1.5 GHz from the mixer output was amplified by a low-noise HEMT amplifier with a 500-MHz bandwidth. A standard *Y*-factor method was used for the noise measurements. No corrections were made for losses in front of the receiver.

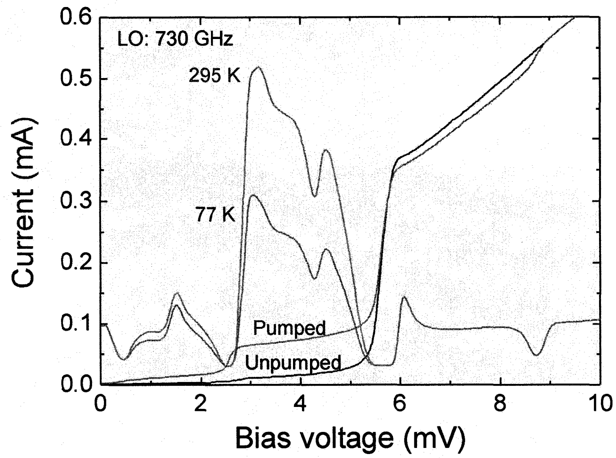

Fig. 8. Heterodyne response of receiver at 730 GHz. Shown are I-V characteristics of mixer with two half-wave SIS junctions with and without LO power. Also shown is IF power as a function of bias voltage for hot (295 K) and cold (77 K) loads.

Figure 8 shows a typical heterodyne response of the receiver at 730 GHz. Since the current density was fairly low, high-quality *I-V* characteristics with a large subgap-to-normal resistance ratio of about 15 were observed when no LO power was applied. Since the fabricated NbN junctions had a large gap voltage of about 5.6 mV, corresponding to 1.35 THz, a first voltage step by photon-assisted tunneling with 730-GHz irradiation clearly appeared at about half the gap voltage. Even though the current density was lower than the design value of 16 kA/cm^2, we observed distinct IF responses to hot and cold loads, indicating that the maximum *Y*-factor was 1.80 at a bias voltage of about 4 mV, corresponding to the double-side-band (DSB) receiver noise temperature of 195 K (about 6 hf/k_B, where h, f, and k_B are the Planck constant, frequency, and Boltzmann constant).

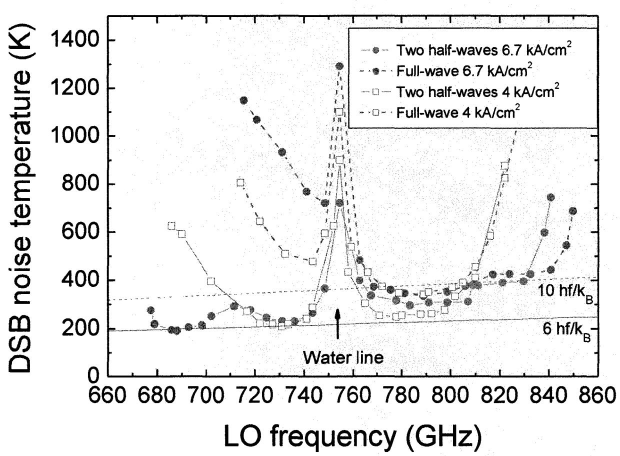

Fig. 9. DSB receiver noise temperature as a function of LO frequency. A 9-μm-thick Mylar beam splitter was used at all measured frequencies.

Figure 9 plots the DSB receiver noise temperature using the tuning circuit as a function of LO frequency. Although the measured center frequency was slightly lower than the design frequency of 870 GHz, a noise temperature below 10 hf/k_B was achieved between 710 and 810 GHz, corresponding to a fractional bandwidth of about 13%. It should be noted that the estimated $\omega C_J R_N$ product is about 37 using the parameters in Table 1. Also plotted in Fig. 9 is the dependence of receiver noise temperature on frequency when a conventional full-wave junction fabricated on the same substrate was used. The fractional tuning bandwidth with the two half-wave junctions was broader than that with the full-wave junction. In the figure, we also plotted the noise temperatures of other mixers with the current density of 6.7 kA/cm^2 that have been measured previously [3]. The noise temperature below 10 hf/k_B exhibited broadband characteristics from 675 to 830 GHz for the two-half-waves. The fractional bandwidth reached 20%, which also was broader than that with the full-wave junction as well as the results with 4 kA/cm^2. This suggests that new tuning method we developed is effective in reducing the current density of the junctions compared to the conventional method, as we had expected from the theoretical-design considerations.

5. Conclusion

We have developed a method of analytically designing a novel tuning circuit with two half-wave distributed junctions using a simplified circuit model, which uniquely determined the circuit parameters without having to depend on the experience of the designer. We theoretically derived a minimum current density, when actually designing the mixer, which is necessary for two-distributed-junction tuning circuit, and the value was much lower than that needed for a conventional tuning circuit. Experimental results using NbN-based SIS mixers supported our theoretical-design considerations. We feel certain that this type of mixer will improve performance at terahertz frequencies.

Acknowledgements

This work was supported in part by the ALMA Joint Research Fund of the National Astronomical Observatory of Japan.

References

[1] Y. Uzawa, A. Kawakami, S. Miki, and Z. Wang: IEEE Trans. Appl. Supercond. **11** (2001) 183.
[2] Y. Uzawa, M. Takeda, and Z. Wang: Jpn. J. Appl. Phys. **42** (2003) 91.
[3] Y. Uzawa, M. Takeda, A. Kawakami, and Z. Wang: Int. J. Infrared Millimeter Wave **24** (2003) 1749.
[4] R. E. Collin: *Foundations for Microwave Engineering* (McGraw-Hill, Inc., 1992) 2nd ed., Chap. 5, p.303.
[5] J. Zmuidzinas, N. G. Ugras, D. Miller, M. Gaidis, H. G. LeDuc, and J. A. Stern: IEEE Trans. Appl. Supercond. **5** (1995) 3053.
[6] A. Kawakami, Z. Wang, and S. Miki: IEEE Trans. Appl. Supercond. **11** (2001) 80.
[7] A. Kawakami, Z. Wang, and S. Miki: J. Appl. Phys. **90** (2001) 4796.
[8] Z. Wang, Y. Uzawa, and A. Kawakami: IEEE Trans. Appl. Supercond. **7** (1997) 2797.
[9] Y. Uzawa and Z. Wang, *Studies of High Temperature Superconductor*, ed. A. V. Narliker (Nova Science, Hauppauge, NY, 2002) Vol. 43, Chap. 9, p. 255.
[10] D. C. Mattis and J. Bardeen, Phys. Rev. **111** (1958) 412.
[11] T. Matsunaga, C. E. Tong, T. Noguchi, and R. Blundell: IEICE Trans. Electron. **E85-C** (2002) 738.
[12] Y. Uzawa, Z. Wang, and A. Kawakami: Appl. Supercond. **6** (1998) 465.